

Capacity-CRB Tradeoff in OFDM Integrated Sensing and Communication Systems

Zhe Huang*, An liu[†], Rui Du[‡] and Tony Xiao Han[§]

*College of Information Science and Electronic Engineering, Zhejiang University, Zhejiang, China
Email: exploer_huangzhe@zju.edu.cn

[†]College of Information Science and Electronic Engineering, Zhejiang University, Zhejiang, China
Email: anliu@zju.edu.cn

[‡]Huawei Technologies Co., Ltd., China
Email: ray.du@huawei.com

[§]Huawei Technologies Co., Ltd., China
Email: tony.hanxiao@huawei.com

Abstract—Integrated sensing and communication (ISAC) has emerged as a key technology for future communication systems. In this paper, we provide a general framework to reveal the fundamental tradeoff between sensing and communication in OFDM systems, where a unified ISAC waveform is exploited to perform both tasks. In particular, we define the Capacity-Bayesian Cramer Rao Bound (BCRB) region in the asymptotically case when the number of subcarriers is large. Specifically, we show that the asymptotically optimal input distribution that achieves the Pareto boundary point of the Capacity-BCRB region is Gaussian and the entire Pareto boundary can be obtained by solving a convex power allocation problem. Moreover, we characterize the structure of the sensing-optimal power allocation in the asymptotically case. Finally, numerical simulations are conducted to verify the theoretical analysis and provide useful insights.

Index Terms—Integrated sensing and communication, Fundamental tradeoff, Capacity-BCRB region.

I. INTRODUCTION

Future 6G communication system will integrate radar sensing and communication functions to support various important application scenarios, such as autonomous driving and smart cities [1], [2]. Under such a background, integrated sensing and communication (ISAC), in which communication signals are exploited to simultaneously achieve high-speed communication and high-accuracy sensing, has emerged as a key technology for future communication systems [1], [2].

As the first step of the research on ISAC, it is necessary to investigate the fundamental performance limits of ISAC and to quantify the optimal tradeoff between sensing accuracy and communication rate for a given ISAC scenario. Recently, a number of works have been dedicated to studying the fundamental limits of ISAC, see, e.g., [3], [4]. A notion of capacity-distortion function built on rate-distortion theory is introduced in [3], [4] for discrete memoryless channels (DMC). The sensing accuracy is quantified by general distortion functions while the communication performance is still quantified by classic communication rate. However, the DMC model is oversimplified to capture the key features of practical ISAC systems. For example, in practice, the sensing state such as the delay/range of the target is not i.i.d. and more complicated physical layer technologies such as MIMO/OFDM are widely used in 5G and beyond systems.

Moreover, it is often difficult to analyze/calculate the exact distortion for a practical system, and we have to resort to various lower bounds of the distortion such as the Bayesian Cramer Rao Bound (BCRB) for tractable analysis. As such, it is practically important to study the capacity-BCRB tradeoff in MIMO/OFDM ISAC systems [5], [6].

In this paper, we consider a mono-static OFDM ISAC system, where the BS serves a mobile user while detecting targets using the same OFDM waveform. For clarity, we focus on the single-input single-output (SISO) OFDM ISAC systems since the capacity-BCRB tradeoff for the SISO case is still open. There are some early attempts to study the capacity-CRB\BCRB tradeoff in MIMO ISAC system, see, e.g., [5], [6]. However, in [5] the authors only capture the optimal input distribution for the communication-optimal and sensing-optimal boundary points and in [6] the authors assume the optimal input distribution is Gaussian without providing a rigorous proof. To overcome these drawbacks, in this paper we establish the Capacity-BCRB region for OFDM ISAC system in the asymptotically case when the number of subcarriers is large. Specifically, we show that the asymptotically optimal input distribution that achieves the Pareto boundary point of the Capacity-BCRB region is Gaussian and the entire Pareto boundary can be obtained by solving a convex power allocation problem. Moreover, we characterized the structure of the sensing-optimal power allocation in the asymptotically case. Finally, numerical simulations are conducted to verify the theoretical analysis and provide useful insights.

II. SYSTEM MODEL AND PERFORMANCE METRICS

A. System Model

Consider an OFDM ISAC system with one BS serving a mobile user while detecting K targets indexed by $k \in \{1, \dots, K\}$. The system consists of a single-antenna BS with N subcarriers and a single-antenna user. Assume a block fading channel model where both the radar target parameters and communication channel remain constant within M OFDM symbol durations.

In the m -th symbol duration, the BS transmits a frequency domain symbol $\mathbf{x}_m \in \mathbb{C}^N$, and the corresponding echo signal in the frequency domain can be expressed as

$$\mathbf{y}_m^r = \text{diag}(\mathbf{x}_m) \mathbf{h}^r + \mathbf{n}_m^r, \quad (1)$$

where $\mathbf{h}^r \in \mathbb{C}^N$ is the radar channel vector and $\mathbf{n}_m^r \sim \mathcal{CN}(0, (\sigma^r)^2 \mathbf{I}) \in \mathbb{C}^N$ is the additive white Gaussian noise (AWGN) with variance $(\sigma^r)^2$. The radar channel vector depends on the delays and radar cross sections (RCSs) of the targets and can be modeled as

$$\mathbf{h}^r = \sum_{k=1}^K \alpha_k^r \boldsymbol{\varphi}(\tau_k^r), \quad (2)$$

where τ_k^r and α_k^r are the delay and RCS of the k -th target, and $\boldsymbol{\varphi}(\tau) \in \mathbb{C}^N$ is given by

$$\boldsymbol{\varphi}(\tau) = [1, e^{-j2\pi f_0 \tau}, \dots, e^{-j2\pi(N-1)f_0 \tau}]^T, \quad (3)$$

where f_0 is the subcarrier spacing. The received frequency-domain communication signal at the user can be expressed as

$$\mathbf{y}_m^c = \text{diag}(\mathbf{x}_m) \mathbf{h}^c + \mathbf{n}_m^c, \quad (4)$$

where $\mathbf{h}^c \in \mathbb{C}^N$ is the communication channel vector and $\mathbf{n}_m^c \sim \mathcal{CN}(0, (\sigma^c)^2 \mathbf{I}) \in \mathbb{C}^N$ is the AWGN.

For convenience, define the aggregation of all the unknown sensing parameters for the K targets as $\boldsymbol{\theta}^r \triangleq [(\boldsymbol{\theta}_1^r)^T \dots (\boldsymbol{\theta}_K^r)^T]^T$ and $\boldsymbol{\theta}_k^r \triangleq [\text{Re}(\alpha_k^r), \text{Im}(\alpha_k^r), \tau_k^r]^T$.

Define the aggregation of all the transmitted symbols as $\mathbf{x} \triangleq [(\mathbf{x}_1)^T \dots (\mathbf{x}_M)^T]^T$, the aggregation of all the echo signal $\mathbf{y}^r \triangleq [(\mathbf{y}_1^r)^T \dots (\mathbf{y}_M^r)^T]^T$ and the aggregation of all the downlink signal $\mathbf{y}^c \triangleq [(\mathbf{y}_1^c)^T \dots (\mathbf{y}_M^c)^T]^T$.

We assume that the BS knows the communication channel vector \mathbf{h}^c from the channel estimation stage and certain prior information $p_{\boldsymbol{\theta}^r}(\boldsymbol{\theta}^r)$ about the target parameters $\boldsymbol{\theta}^r$ from e.g., the sensing results in the previous block (assuming the target parameters of adjacent blocks are correlated according to certain probability model). The transmitted frequency domain data symbol \mathbf{x}_m is known to the BS but unknown to the user. Moreover, $\mathbf{x}_m, m = 1, \dots, M$ are *i.i.d.* over different symbols for certain input distribution $p_{\mathbf{X}}$, i.e. $p_{\mathbf{X}}(\mathbf{x}) = \prod_{m=1}^M p_{\mathbf{X}}(\mathbf{x}_m)$.

Note that for clarity, we focus on the range/delay estimation of the targets for sensing, and thus it is sufficient to consider a wideband single-input single-output (SISO) systems since the delay estimation performance is mainly determined by the system bandwidth. In a wideband multiple-input-multiple-output (MIMO) ISAC system with Angle of arrival (AoA) and Doppler estimation capability, the model in (2) should also include the AoA and Doppler of the target's paths, which is left as future work.

B. Capacity-Distortion and Capacity-CRB Tradeoff

The capacity-distortion function $C(D)$ represents the tradeoff between communication capacity and sensing distortion for ISAC systems. In this section, we study the optimal capacity-distortion tradeoff $C(D)$ for the above OFDM-ISAC system as illustrated in Fig. 1. Specifically, we choose the sensing distortion metric $e(\boldsymbol{\theta}^r, \hat{\boldsymbol{\theta}}^r)$ as the mean squared error (MSE), i.e., $e(\boldsymbol{\theta}^r, \hat{\boldsymbol{\theta}}^r) = \|\boldsymbol{\theta}^r - \hat{\boldsymbol{\theta}}^r\|^2$, where $\hat{\boldsymbol{\theta}}^r$ is the estimator of $\boldsymbol{\theta}^r$. In this case, for any given transmit signal \mathbf{x} and received echo signal \mathbf{y}^r , the optimal estimator for $\boldsymbol{\theta}^r$ is given by the minimum MSE (MMSE) estimator as [7]

$$\hat{\boldsymbol{\theta}}^r(\mathbf{y}^r, \mathbf{x}) \triangleq \int p(\boldsymbol{\theta}^r | \mathbf{y}^r, \mathbf{x}) \boldsymbol{\theta}^r d\boldsymbol{\theta}^r. \quad (5)$$

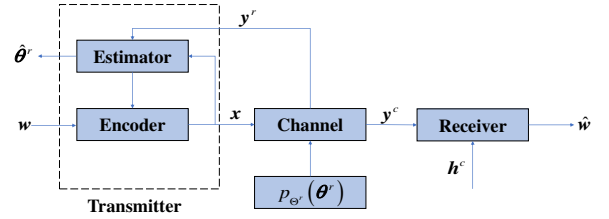


Fig. 1. A point-to-point OFDM-ISAC channel.

Following similar analysis as in [3], [4], the optimal capacity-distortion of the OFDM ISAC system considered is given by

$$\mathcal{P} : C(D) = \max_{p_{\mathbf{X}}} I(\mathbf{Y}^c; \mathbf{X}), \quad (6a)$$

$$\text{s.t.} \quad \int p_{\mathbf{X}}(\mathbf{x}) d\mathbf{x} = 1, \quad (6b)$$

$$\int p_{\mathbf{X}}(\mathbf{x}) \|\mathbf{x}\|^2 d\mathbf{x} \leq P, \quad (6c)$$

$$\int p_{\mathbf{X}}(\mathbf{x}) c(\mathbf{x}) d\mathbf{x} \leq D, \quad (6d)$$

where $I(\mathbf{Y}^c; \mathbf{X})$ is the mutual information between \mathbf{Y}^c and \mathbf{X} , P is the total transmitted power, D is the maximum tolerated distortion, $c(\mathbf{x}) \triangleq \iint p(\mathbf{y}^r | \mathbf{x}, \boldsymbol{\theta}^r) p_{\boldsymbol{\theta}^r}(\boldsymbol{\theta}^r) e(\boldsymbol{\theta}^r, \hat{\boldsymbol{\theta}}^r) d\mathbf{y}^r d\boldsymbol{\theta}^r$ is the average MSE for given transmit signal \mathbf{x} , and the joint distribution of random variables $\{\mathbf{Y}^r \mathbf{Y}^c \mathbf{X} \boldsymbol{\theta}^r\}$ is given by

$$p_{\boldsymbol{\theta}^r}(\boldsymbol{\theta}^r) p_{\mathbf{X}}(\mathbf{x}) p(\mathbf{y}^c | \mathbf{x}) p(\mathbf{y}^r | \mathbf{x}, \boldsymbol{\theta}^r), \quad (7)$$

where $p(\mathbf{y}^r | \mathbf{x}, \boldsymbol{\theta}^r)$ and $p(\mathbf{y}^c | \mathbf{x})$ are the Gaussian channel transition probabilities determined by (1) and (4), respectively.

In general, it is difficult to obtain the closed-form expressions of the MMSE estimator and the relevant MMSE. It is well-known that certain practical estimators are capable of approaching the Bayesian Cramer-Rao Bound (BCRB) when the $\text{SNR}^r \triangleq P(\sigma^r)^{-2}$ is sufficiently high [7], so we choose the BCRB as an alternative way to evaluate the distortion.

Therefore, we can replace the term $c(\mathbf{x})$ with its BCRB $\tilde{c}(\mathbf{x})$ as

$$\tilde{c}(\mathbf{x}) \triangleq \text{Tr} \left\{ \left[\mathbb{E}_{\Theta^r} [\mathbf{J}^o(\mathbf{x})] + \mathbf{J}^p \right]^{-1} \right\}, \quad (8)$$

where the Fisher Information Matrices (FIMs) $\mathbf{J}^o(\mathbf{x})$ and \mathbf{J}^p are given by

$$\mathbf{J}^o(\mathbf{x}) \triangleq \mathbb{E}_{\Theta^r} \left[\mathbf{g}^o(\boldsymbol{\theta}^r) \mathbf{g}^o(\boldsymbol{\theta}^r)^T \right], \quad (9)$$

$$\mathbf{J}^p \triangleq \mathbb{E}_{\Theta^r} \left[\mathbf{g}^p(\boldsymbol{\theta}^r) \mathbf{g}^p(\boldsymbol{\theta}^r)^T \right], \quad (10)$$

where $\mathbf{g}^o(\boldsymbol{\theta}^r) \triangleq \nabla_{\boldsymbol{\theta}^r} (\ln p(\mathbf{y}^r | \boldsymbol{\theta}^r, \mathbf{x}))$, $\mathbf{g}^p(\boldsymbol{\theta}^r) \triangleq \nabla_{\boldsymbol{\theta}^r} (\ln p_{\Theta^r}(\boldsymbol{\theta}^r))$. Then the capacity-BCRB tradeoff $\tilde{C}(D)$ is given by replacing the $c(\mathbf{x})$ in (6d) with its BCRB $\tilde{c}(\mathbf{x})$.

Note that the exact CRB in (8) exhibits a rather complicated dependence on the frequency domain symbol \mathbf{x} . Thus, it does not provide immediate insights on the estimation accuracy. To remedy this problem, we derive the asymptotic CRB (ACRB) as $N \rightarrow \infty$ in the next section. The latter will be a much simpler function of the frequency domain symbol \mathbf{x} . Therefore, the ACRB is an interesting tool to evaluate the influence of the frequency domain symbol \mathbf{x} on the estimation performance.

III. ASYMPTOTIC CRAMER RAO BOUND ANALYSIS

In this section, we derive the exact BCRB and the ACRB.

A. Derivation of the exact BCRB

By definition, the $\mathbf{J}^o(\mathbf{x})$ can be decomposed as

$$\mathbf{J}^o(\mathbf{x}) = \begin{bmatrix} \mathbf{J}_{11}^o(\mathbf{x}) & \cdots & \mathbf{J}_{1K}^o(\mathbf{x}) \\ \vdots & \ddots & \vdots \\ \mathbf{J}_{1K}^o(\mathbf{x})^T & \cdots & \mathbf{J}_{KK}^o(\mathbf{x}) \end{bmatrix}, \quad (11)$$

where $\mathbf{J}_{kl}^o(\mathbf{x}) \triangleq \sum_m (\mathbf{J}_{mkl}^o(\mathbf{x}))$, $\forall k, l$ and the (p, q) -th element of the submatrix $\mathbf{J}_{mkl}^o(\mathbf{x})$ is given by

$$[\mathbf{J}_{mkl}^o(\mathbf{x})]_{pq} = 2(\sigma^r)^{-2} \text{Re} \left[\left(\frac{\partial \boldsymbol{\mu}_m^r}{\partial \theta_{kp}^r} \right)^H \left(\frac{\partial \boldsymbol{\mu}_m^r}{\partial \theta_{lq}^r} \right) \right], \quad (12)$$

where $\boldsymbol{\mu}_m^r \triangleq \text{diag}(\mathbf{x}_m) \mathbf{h}^r$ and $p, q \in \{1, 2, 3\}$. After some straightforward calculation, the (k, k) -th submatrix $\mathbf{J}_{mkk}^o(\mathbf{x})$ and (k, l) -th submatrix $\mathbf{J}_{mkl}^o(\mathbf{x})$ are given in by (13) and (14).

$$\mathbf{J}_{mkk}^o(\mathbf{x}) = 2(\sigma^r)^{-2} \begin{bmatrix} (\mathbf{J}_{mkk}^o)_{11} & (\mathbf{J}_{mkk}^o)_{12} \\ (\mathbf{J}_{mkk}^o)_{12}^T & (\mathbf{J}_{mkk}^o)_{22} \end{bmatrix}, \quad (13)$$

$$\mathbf{J}_{mkl}^o(\mathbf{x}) = 2(\sigma^r)^{-2} \begin{bmatrix} (\mathbf{J}_{mkl}^o)_{11} & (\mathbf{J}_{mkl}^o)_{12} \\ (\mathbf{J}_{mkl}^o)_{21} & (\mathbf{J}_{mkl}^o)_{22} \end{bmatrix}, \quad (14)$$

The sub-matrices in $\mathbf{J}_{mkk}^o(\mathbf{x})$ and $\mathbf{J}_{mkl}^o(\mathbf{x})$ are given as

$$(\mathbf{J}_{mkk}^o)_{11} \triangleq \text{diag}(U_{mk}, U_{mk}), \quad (15a)$$

$$(\mathbf{J}_{mkk}^o)_{12} \triangleq [\text{Im}(\alpha_k^r T_{mk}), -\text{Re}(\alpha_k^r T_{mk})]^T, \quad (15b)$$

$$(\mathbf{J}_{mkk}^o)_{22} \triangleq \omega_0^2 |\alpha_k^r|^2 V_{mk}, \quad (15c)$$

$$(\mathbf{J}_{mkl}^o)_{12} \triangleq [\text{Im}(\alpha_l^r T_{mkl}), -\text{Re}(\alpha_l^r T_{mkl})]^T, \quad (15d)$$

$$(\mathbf{J}_{mkl}^o)_{21} \triangleq [\text{Im}(\alpha_k^r T_{mkl}), -\text{Re}(\alpha_k^r T_{mkl})]^T, \quad (15e)$$

$$(\mathbf{J}_{mkl}^o)_{22} \triangleq \omega_0^2 (\alpha_k^r)^* \alpha_l^r V_{mkl}, \quad (15f)$$

$$(\mathbf{J}_{mkl}^o)_{11} \triangleq \begin{bmatrix} \text{Re}(U_{mkl}) & -\text{Im}(U_{mkl}) \\ \text{Im}(U_{mkl}) & \text{Re}(U_{mkl}) \end{bmatrix}, \quad (15g)$$

where $\omega_0 \triangleq 2\pi f_0$.

The collection of $\{U_{mk}, U_{mkl}, T_{mk}, T_{mkl}, V_{mk}, V_{mkl}\}_{m,k,l}$ are given as

$$U_{mk} = \sum_n |x_{nm}|^2, \quad (16a)$$

$$U_{mkl} = \sum_n |x_{nm}|^2 e^{j\omega_0(n-1)\bar{\tau}_{kl}^r}, \quad (16b)$$

$$T_{mk} = \sum_n (n-1) |x_{nm}|^2, \quad (16c)$$

$$T_{mkl} = \sum_n (n-1) |x_{nm}|^2 e^{j\omega_0(n-1)\bar{\tau}_{kl}^r}, \quad (16d)$$

$$V_{mk} = \sum_n (n-1)^2 |x_{nm}|^2, \quad (16e)$$

$$V_{mkl} = \sum_n (n-1)^2 |x_{nm}|^2 e^{j\omega_0(n-1)\bar{\tau}_{kl}^r}, \quad (16f)$$

where $\bar{\tau}_{kl}^r \triangleq \tau_k^r - \tau_l^r$.

B. Derivation of the ACRB

It can be observed that the elements in $\mathbf{J}_{mkk}^o(\mathbf{x})$ and $\mathbf{J}_{mkl}^o(\mathbf{x})$ relies on the realizations of the random variable \mathbf{x}_m which is hard to evaluate. Motivated by the classical strong law of large numbers (SLLN) that the sample mean of *i.i.d* random variables converges to its mean almost surely, we seek to derive the asymptotic behaviors. Note that the *i.i.d* assumption may not be valid since the sample from different subcarriers may be correlated. To overcome this technical challenge, let us introduce the following lemma, which is proved in [8].

Lemma 1. *Let $\{w_n\}$ denotes a non-negative deterministic sequence and $\{Z_n\}$ denotes a random non-negative sequence with finite variance. Define*

$$W_N \triangleq \sum_n w_n, T_N \triangleq \sum_n w_n Z_n.$$

Under the technical conditions claimed in [8], we have the following generalized SLLN holds

$$\frac{T_N - \mathbb{E}[T_N]}{W_N} \rightarrow 0, a.s. \quad (17)$$

In order to obtain the following corollary, we shall also have some assumptions on P_{nm} which is given as follow,

$$0 \leq P_{nm} \leq P_{max}, \forall n, m \quad (18)$$

where $P_{nm} = \mathbb{E} \left[|x_{nm}|^2 \right]$ denotes the transmitted power on n -th subcarrier in the m -th symbol duration. Note that the constraint $P_{nm} \leq P_{max}$ for certain P_{max} with order $O\left(\frac{P}{NM}\right)$ is widely used in practice, because such a constraint will ensure the non-zero communication rate at each subcarrier for communication and avoid impractical power allocation by directly minimizing the CRB without any constraint for sensing [9], [10].

Substituting $Z_n = |x_{nm}|^2$, $w_n^s \triangleq (n-1)^s$, $s \in \{0, 1, 2\}$ into the generalized SLLN in Lemma 1, we can prove the following Corollary. The detailed proof is omitted due to space limit.

Corollary 1. Let $w_n^s \triangleq (n-1)^s$, where $s \in \{0, 1, 2\}$. We have

$$\frac{U_{mk} - \bar{U}_{mk}}{\sum_n w_n^0} \rightarrow 0, \quad a.s. \quad (19a)$$

$$\frac{T_{mk} - \bar{T}_{mk}}{\sum_n w_n^1} \rightarrow 0, \quad a.s. \quad (19b)$$

$$\frac{V_{mk} - \bar{V}_{mk}}{\sum_n w_n^2} \rightarrow 0, \quad a.s. \quad (19c)$$

where $\bar{U}_{mk} \triangleq \mathbb{E}[U_{mk}] = \sum_n w_n^0 P_{nm}$, $\bar{T}_{mk} \triangleq \mathbb{E}[T_{mk}] = \sum_n w_n^1 P_{nm}$, $\bar{V}_{mk} \triangleq \mathbb{E}[V_{mk}] = \sum_n w_n^2 P_{nm}$.

Similarly, let $\tilde{w}_n^s \triangleq (n-1)^s e^{j\omega_0(n-1)\tau_{kl}^r}$. We have

$$\frac{U_{mkl} - \bar{U}_{mkl}}{\sum_n \tilde{w}_n^0} \rightarrow 0, \quad a.s. \quad (20a)$$

$$\frac{T_{mkl} - \bar{T}_{mkl}}{\sum_n \tilde{w}_n^1} \rightarrow 0, \quad a.s. \quad (20b)$$

$$\frac{V_{mkl} - \bar{V}_{mkl}}{\sum_n \tilde{w}_n^2} \rightarrow 0, \quad a.s. \quad (20c)$$

where $\bar{U}_{mkl} \triangleq \mathbb{E}[U_{mkl}] = \sum_n \tilde{w}_n^0 P_{nm}$, $\bar{T}_{mkl} \triangleq \mathbb{E}[T_{mkl}] = \sum_n \tilde{w}_n^1 P_{nm}$, $\bar{V}_{mkl} \triangleq \mathbb{E}[V_{mkl}] = \sum_n \tilde{w}_n^2 P_{nm}$.

Define the asymptotic normalized FIM (ANFIM) as $\bar{\mathbf{J}}^o(\mathbf{x}) \triangleq \lim_{N \rightarrow \infty} \mathbf{L} \mathbf{J}^o(\mathbf{x}) \mathbf{L}^T$, where

$$\mathbf{L} \triangleq \text{blkdiag}(\mathbf{L}_1, \dots, \mathbf{L}_K), \quad (21)$$

with $\mathbf{L}_k \triangleq \text{diag}\left(N^{-\frac{1}{2}}M^{-\frac{1}{2}}, N^{-\frac{1}{2}}M^{-\frac{1}{2}}, N^{-\frac{3}{2}}M^{-\frac{1}{2}}\right)$, $\forall k$.

Corollary 2. Under assumptions in (18), the ANFIM is given by (22), where $\bar{\mathbf{J}}_{kl}^o(\mathbf{x}) \triangleq \sum_m (\bar{\mathbf{J}}_{mkl}^o(\mathbf{x}))$, $\forall m, k, l$ and $\bar{\mathbf{J}}_{mkl}^o(\mathbf{x}) \triangleq \lim_{N \rightarrow \infty} \mathbf{L}_k \mathbf{J}_{mkl}^o(\mathbf{x}) \mathbf{L}_l^T$, $\forall m, k, l$. Moreover, the Big O order of elements in $\bar{\mathbf{J}}_{kk}^o(\mathbf{x})$ and $\bar{\mathbf{J}}_{kl}^o(\mathbf{x})$, $\forall k, l, p, q$ are given by equation (23a) -(23e) and (24).

$$\bar{\mathbf{J}}^o(\mathbf{x}) \triangleq \begin{bmatrix} \bar{\mathbf{J}}_{11}^o(\mathbf{x}) & \cdots & \bar{\mathbf{J}}_{1K}^o(\mathbf{x}) \\ \vdots & \ddots & \vdots \\ \bar{\mathbf{J}}_{1K}^o(\mathbf{x})^T & \cdots & \bar{\mathbf{J}}_{KK}^o(\mathbf{x}) \end{bmatrix}, \quad (22)$$

$$O[\bar{\mathbf{J}}_{kk}^o(\mathbf{x})]_{11} = O[\bar{\mathbf{J}}_{kk}^o(\mathbf{x})]_{22} = P_{max}, \quad (23a)$$

$$O[\bar{\mathbf{J}}_{kk}^o(\mathbf{x})]_{12} = O[\bar{\mathbf{J}}_{kk}^o(\mathbf{x})]_{21} = 0, \quad (23b)$$

$$O[\bar{\mathbf{J}}_{kk}^o(\mathbf{x})]_{13} = O[\bar{\mathbf{J}}_{kk}^o(\mathbf{x})]_{13} = \frac{1}{2} \tilde{\alpha}_k^r P_{max}, \quad (23c)$$

$$O[\bar{\mathbf{J}}_{kk}^o(\mathbf{x})]_{23} = O[\bar{\mathbf{J}}_{kk}^o(\mathbf{x})]_{32} = -\frac{1}{2} \bar{\alpha}_k^r P_{max}, \quad (23d)$$

$$O[\bar{\mathbf{J}}_{kk}^o(\mathbf{x})]_{33} = \frac{1}{3} \left(|\tilde{\alpha}_k^r|^2 + |\bar{\alpha}_k^r|^2 \right) P_{max}, \quad (23e)$$

$$O \left\{ \frac{[\bar{\mathbf{J}}_{kl}^o(\mathbf{x})]_{pq}}{[\bar{\mathbf{J}}_{kk}^o(\mathbf{x})]_{pq}} \right\} = \frac{1}{N}, \quad \forall p, q \in \{1, 2, 3\}, \quad (24)$$

where $\tilde{\alpha}_k^r \triangleq \omega_0 \text{Im}(\alpha_k^r)$ and $\bar{\alpha}_k^r \triangleq \omega_0 \text{Re}(\alpha_k^r)$.

Proof: Equation (23a) - (24) are derived using the fact that for any $t \in \{0, 1, 2\}$, the Big O order for the general expression of elements in $\bar{\mathbf{J}}_{kk}^o(\mathbf{x})$ and $\bar{\mathbf{J}}_{kl}^o(\mathbf{x})$, $\forall k, l, p, q$ is given by (25) [11], where $\omega_{kl} \triangleq \omega_0(\tau_k^r - \tau_l^r)$. The other calculation is straightforward and omitted due to space limit. \blacksquare

Therefore, $\bar{\mathbf{J}}^o(\mathbf{x})$ will tend to be a block-diagonal matrix with negligible approximation error as shown in (26).

$$\lim_{N \rightarrow \infty} \frac{\|\bar{\mathbf{J}}^o(\mathbf{x}) - \tilde{\mathbf{J}}^o(\mathbf{x})\|_F^2}{\|\bar{\mathbf{J}}^o(\mathbf{x})\|_F^2} = 0, \quad (26)$$

where $\tilde{\mathbf{J}}^o(\mathbf{x}) \triangleq \text{blkdiag}[\bar{\mathbf{J}}_{11}^o(\mathbf{x}), \dots, \bar{\mathbf{J}}_{KK}^o(\mathbf{x})]$.

It can be observed that $\bar{\mathbf{J}}^o(\mathbf{x})$ does not depend on exact input distribution $p_{\mathbf{X}}(\mathbf{x})$ but only depends on the power allocation of all subcarriers. Therefore, we can rewrite $\bar{\mathbf{J}}^o(\mathbf{x})$ as a function of the aggregated power allocation vector $\mathbf{p} \triangleq [\mathbf{p}_1^T, \dots, \mathbf{p}_M^T]^T$: $\bar{\mathbf{J}}^o(\mathbf{p})$, where $\mathbf{p}_m \triangleq [P_{1m}, \dots, P_{nm}]^T$ is the power allocation vector for the m -th symbol. Then we are ready to define the ACRB as a function of \mathbf{p} :

$$\text{ACRB}(\mathbf{p}) \triangleq \text{Tr} \left\{ \left[\mathbb{E}_{\Theta^r} [\hat{\mathbf{J}}(\mathbf{x})] + \mathbf{J}^p(\theta^r) \right]^{-1} \right\}. \quad (27)$$

where $\hat{\mathbf{J}}(\mathbf{x}) \triangleq \mathbf{L}^{-T} \bar{\mathbf{J}}^o(\mathbf{x}) \mathbf{L}^{-1}$. From the above analysis, it is easy to see that ACRB is a good approximation of BCRB for large N . Therefore, for large N , we may study the capacity-ACRB tradeoff as a good approximation for the capacity-BCRB tradeoff function.

IV. CAPACITY-BCRB REGION ANALYSIS

In general, the capacity-BCRB region takes the form illustrated in Fig. 2. The convex hull of the points $(+\infty, 0)$, $(+\infty, C_{max})$, $(D_{min}, 0)$ constitutes an inner bound of the capacity-distortion region, where $P_s \triangleq (D_{min}, C_{min})$ is the sensing-optimal (S-optimal) point and $P_c \triangleq (D_{max}, C_{max})$ is the communication-optimal (C-optimal) point. The line segment connecting P_s and P_c can be achieved using the time-sharing scheme which allocates orthogonal resources for sensing and communication.

In general, it is very hard to capture the exact boundary of the capacity-BCRB region (i.e., the red boundary in Fig. 2) for finite N . In the following theorem, we characterize the asymptotically optimal input distribution that can achieve the

$$O \left\{ \frac{1}{N^t M P_{max}} \sum_n \sum_m (n-1)^t P_{nm} e^{j\omega_{kl}(n-1)} \right\} = \begin{cases} \frac{1}{t+1} + O\left(\frac{1}{N}\right), & \omega_{kl} = 0, k = l \\ O\left(\frac{1}{N}\right), & \omega_{kl} \neq 0, k \neq l \end{cases}, \quad (25)$$

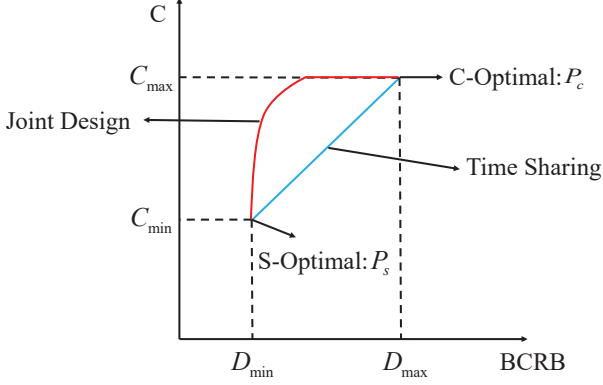


Fig. 2. The Capacity-BCRB Regions for OFDM-ISAC system

boundary of the capacity-BCRB region for sufficient large N ($N \rightarrow \infty$).

Theorem 1. *As $N \rightarrow \infty$, the asymptotic optimal input distribution $p_{\mathbf{X}}(\mathbf{x})$ for the optimization problem \mathcal{P} is Gaussian distribution with zero mean, and thus Problem \mathcal{P} reduces to a power allocation problem as*

$$\bar{\mathcal{P}} : \bar{C}(D) = \max_{\mathbf{p}} f(\mathbf{p}), \quad (28a)$$

$$\text{s.t. } l(\mathbf{p}) \triangleq \mathbf{1}^T \mathbf{p} \leq P, \quad (28b)$$

$$d(\mathbf{p}) \triangleq \text{ACRB}(\mathbf{p}) \leq D, \quad (28c)$$

$$0 \leq P_{nm} \leq P_{max}, \quad (28d)$$

where \mathbf{p} is the aggregated power allocation vector, and $f(\mathbf{p}) \triangleq \sum_m \sum_n \log_2 \left(1 + (\sigma^c)^{-2} P_{nm} |h_{nm}^c|^2 \right)$ is the mutual information $\bar{I}(\mathbf{Y}^c; \mathbf{X})$ under the Gaussian input distribution. Moreover, the power allocation problem $\bar{\mathcal{P}}$ is convex.

Proof: It can be observed from (27) that as $N \rightarrow \infty$, the sensing performance only depends on the power allocation of all subcarriers but does not depend the exact input distribution $p_{\mathbf{X}}(\mathbf{x})$. On the other hand, for given power allocation, Gaussian input distribution is optimal for communications. Therefore, the asymptotic optimal input distribution for the optimization problem \mathcal{P} is Gaussian and thus \mathcal{P} reduces to the power allocation problem. Now, let us prove the power allocation problem $\bar{\mathcal{P}}$ is convex.

It is obvious that $f(\mathbf{p})$ is a concave function of \mathbf{p} . Therefore, we only need to prove $d(\mathbf{p}) \triangleq \text{ACRB}(\mathbf{p})$ is a convex function of \mathbf{p} . First, the function $d(\mathbf{p}) = \text{Tr} \left\{ \left[\mathbb{E}_{\Theta^r} [\hat{\mathbf{J}}(\mathbf{x})] + \mathbf{J}^p(\theta^r) \right]^{-1} \right\}$ is a convex function of $\mathbb{E}_{\Theta^r} [\hat{\mathbf{J}}(\mathbf{x})]$. Second, every element in $\mathbb{E}_{\Theta^r} [\hat{\mathbf{J}}(\mathbf{x})]$ is a convex function of \mathbf{p} . Therefore, the function $d(\mathbf{p}) \triangleq \text{ACRB}(\mathbf{p})$ is a convex function of \mathbf{p} . ■

By Theorem 1, the Pareto optimal boundary of the capacity-BCRB region for large N (or equivalently, the capacity-ACRB region) can be obtained by solving the convex power allocation problem $\bar{\mathcal{P}}$ with different distortion constraint D . Since the communication-optimal power allocation is known to have a water-filling structure, in the following section, we shall focus on study the structure of the S-optimal power allocation that minimizes the ACRB (\mathbf{p}).

V. SENSING-OPTIMAL POWER ALLOCATION

The S-optimal power allocation can be obtained through the following convex optimization problem:

$$\mathcal{P}_s : \min_{\mathbf{p}} d(\mathbf{p}), \quad (29a)$$

$$\text{s.t. } \mathbf{1}^T \mathbf{p} = P, \quad (29b)$$

$$0 \leq P_{nm} \leq P_{max}, \quad (29c)$$

Note that \mathcal{P}_s is still hard to analyze under arbitrarily prior information $p_{\Theta^r}(\theta^r)$, so we add some reasonable technical assumptions to derive the following corollary.

Corollary 3. *Under the assumption that $\mathbb{E}[\alpha_k^r] = 0, \forall k$, $\hat{\mathbf{J}}_{kk}(\mathbf{x}) \triangleq \mathbb{E}_{\Theta^r} \left[\mathbf{L}_k^{-T} \tilde{\mathbf{J}}_{kk}^p(\mathbf{x}) \mathbf{L}_k^{-1} \right]$, $\forall k$ is a diagonal matrix given by (30), where $\tilde{\mathbf{V}}_k \triangleq \sum_{m,n} (n-1)^2 P_{nm}$ and $\sigma_{\alpha_k^r}^2 \triangleq \mathbb{E} \left[|\alpha_k^r|^2 \right]$. Moreover, the prior information matrix $\mathbf{J}^p \triangleq \text{blkdiag} \left[\mathbf{J}_{11}^p, \dots, \mathbf{J}_{KK}^p \right]$ is a block-diagonal matrix, and $\mathbf{J}_{kk}^p, \forall k$ are diagonal matrices determined by the mean vector and covariance matrix of θ^r .*

Proof: The proof follows from straightforward calculations and is omitted due to space limit. ■

Therefore, when $\mathbb{E}[\alpha_k^r] = 0, \forall k$, the ACRB is given by (31), where $\text{ACRB}^{\alpha_k^r}(\mathbf{p})$ and $\text{ACRB}^{\tau_k^r}(\mathbf{p})$ are given by equation (32) and (33), respectively.

$$\hat{\mathbf{J}}_{kk}(\mathbf{x}) = 2(\sigma^r)^{-2} \text{diag} \left[P, P, (\omega_0 \sigma_{\alpha_k^r})^2 \tilde{\mathbf{V}}_k \right], \quad (30)$$

$$\text{ACRB}(\mathbf{p}) = \sum_k \left[\text{ACRB}^{\alpha_k^r}(\mathbf{p}) + \text{ACRB}^{\tau_k^r}(\mathbf{p}) \right], \quad (31)$$

$$\text{ACRB}^{\alpha_k^r}(\mathbf{p}) \triangleq \frac{1}{(\sigma^r)^{-2} P + (\mathbf{J}_{kk}^p)_{11}}, \quad (32)$$

$$\text{ACRB}^{\tau_k^r}(\mathbf{p}) \triangleq \frac{1}{2(\sigma^r)^{-2} (\omega_0 \sigma_{\alpha_k^r})^2 \tilde{\mathbf{V}}_k + (\mathbf{J}_{kk}^p)_{33}}. \quad (33)$$

Theorem 2. *The optimal condition for \mathcal{P}_s under the assumption $\mathbb{E}[\alpha_k^r] = 0, \forall k$ is that*

$$P_{nm} = \begin{cases} P_{max}, & N - N_{act} + 1 \leq n \leq N, \\ \frac{P_c}{M}, & n = N - N_{act}, \\ 0, & n < N - N_{act}, \end{cases}$$

where $P_e = P - P_{max}MN_{act}$, $N_{act} = \left\lceil \frac{P}{MP_{max}} \right\rceil$ and $\lceil \cdot \rceil$ is the ceiling operation.

Proof: It can be observed from equation (31) that the ACRB (p) is minimized when $2(\sigma^r)^{-2}(\omega_0\sigma_{\alpha_k})^2\tilde{V}_k$ is maximized. Theorem 2 means that to achieve the best sensing performance, we must allocate the maximum transmitted power at the N_{act} edge-most subcarriers. ■

VI. SIMULATION RESULTS

In this section, we shall use simulations to compare the communication and sensing tradeoff by varying D and solving $\bar{\mathcal{P}}$ to obtain the capacity ACRB region (C, D). In the simulation figures, we only show the delay estimation error in the x-axis for clarity. The subcarrier spacing f_0 is fixed as 15 KHz.

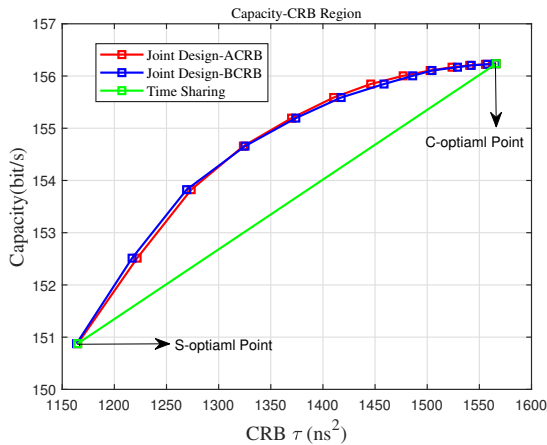


Fig. 3. Capacity-ACRB Region for single target case.

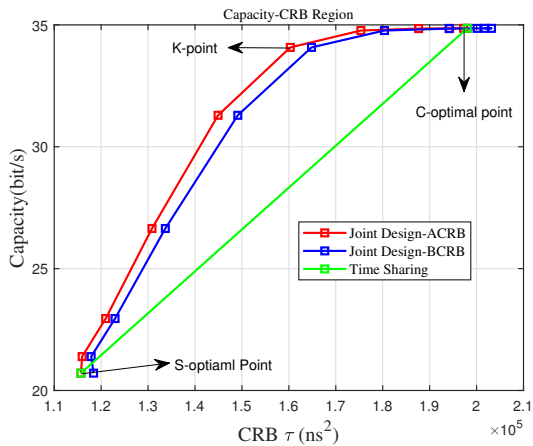


Fig. 4. Capacity-ACRB Region for two target case.

Fig. 3 illustrates the Capacity-BCRB\ACRB Region for the single target case. We set $N = 1024, M = 1$ and the prior information $p_{\Theta^r}(\theta^r)$ as Gaussian distribution. As can be observed, the joint design scheme by solving the convex optimization problem $\bar{\mathcal{P}}$ has significant performance gain compared with the time sharing scheme which allocating orthogonal resources for sensing and communication and the ACRB is a good approximation of BCRB for large N with

negligible approximation error. Moreover, when N is large and there is only a single target, there is almost no tradeoff between communication and sensing, e.g., the capacity loss of the S-optimal point is only about 3% compared to the C-optimal point.

In Fig. 4, we plot the Capacity-BCRB\ACRB Region for the two target case. We set $N = 256, M = 1$, the prior information $p_{\Theta^r}(\theta^r)$ as Gaussian distribution and the difference between the delay of two targets as 523 ns, which is $\frac{2}{Nf_0}$. As can be observed, the joint design scheme still has significant performance gain compared with the time sharing scheme. However, the approximation error of ACRB is larger than the case when $N = 1024$. Moreover, when N is smaller and there are two close targets, there is a tradeoff between communication and sensing, e.g., the capacity loss of the S-optimal point is about 42% compared to the C-optimal point. In this case, it is desirable to operate the ISAC system at the knee point where the communication capacity loss is small and the sensing performance is also relatively good (e.g., the K-point in Fig. 4).

VII. CONCLUSIONS

In this work, we have investigated the fundamental limit of OFDM ISAC system. A Capacity-BCRB optimization problem for such system is formulated. Based on the asymptotic analysis, we show that the asymptotically optimal input distribution that achieves the Pareto boundary point of the Capacity-BCRB region is Gaussian and the entire Pareto boundary can be obtained by solving a convex power allocation problem. Moreover, we characterize the structure of the sensing-optimal power allocation in the asymptotically case under some reasonable technical assumptions. As future work, it is of great interest to extend the current framework to multi-terminal ISAC topologies (such as MACs and BCs).

REFERENCES

- [1] A. Liu, Z. Huang, M. Li, Y. Wan, W. Li, T. X. Han, C. Liu, R. Du, D. K. P. Tan, J. Lu *et al.*, "A survey on fundamental limits of integrated sensing and communication," *IEEE Commun. Surveys Tuts.*, vol. 24, no. 2, pp. 994–1034, 2022.
- [2] F. Liu, C. Masouros, A. P. Petropulu, H. Griffiths, and L. Hanzo, "Joint radar and communication design: Applications, state-of-the-art, and the road ahead," *IEEE Trans. Commun.*, vol. 68, no. 6, pp. 3834–3862, June, 2020.
- [3] Y. Liu, M. Li, A. Liu, J. Lu, and T. X. Han, "Information-theoretic limits of integrated sensing and communication with correlated sensing and channel states for vehicular networks," *IEEE Trans. Veh. Technol.*, vol. 71, no. 9, pp. 10 161–10 166, 2022.
- [4] M. Kobayashi, G. Caire, and G. Kramer, "Joint state sensing and communication: Optimal tradeoff for a memoryless case," in *2018 IEEE International Symposium on Information Theory (ISIT)*. IEEE, 2018, pp. 111–115.
- [5] Y. Xiong, F. Liu, Y. Cui, W. Yuan, and T. X. Han, "Flowing the information from Shannon to Fisher: Towards the fundamental tradeoff in ISAC," *arXiv preprint arXiv:2204.06938*, 2022.
- [6] H. Hua, X. Song, Y. Fang, T. X. Han, and J. Xu, "MIMO integrated sensing and communication with extended target: CRB-rate tradeoff," *arXiv preprint arXiv:2205.14050*, 2022.
- [7] S. M. Kay, *Fundamentals of statistical signal processing: estimation theory*. Prentice-Hall, Inc., 1993.
- [8] V. Petrov, "On stability of sums of nonnegative random variables," *Journal of Mathematical Sciences*, vol. 159, no. 3.
- [9] M. Bică and V. Koivunen, "Radar waveform optimization for target parameter estimation in cooperative radar-communications systems," *IEEE Trans. Aerosp. Electron. Syst.*, vol. 55, no. 5, pp. 2314–2326, 2018.

- [10] S. D. Liyanaarachchi, T. Riihonen, C. B. Barneto, and M. Valkama, "Optimized waveforms for 5G–6G communication with sensing: Theory, simulations and experiments," *IEEE Trans. Wireless Commun.*, vol. 20, no. 12, pp. 8301–8315, 2021.
- [11] O. Besson and P. Stoica, "On parameter estimation of MIMO flat-fading channels with frequency offsets," *IEEE Trans. Signal Processing*, vol. 51, no. 3, pp. 602–613, 2003.